# Multiphoton-magnetophonon resonance in two-dimensional electron systems under intense terahertz fields

S. Y. Liu and X. L. Lei
*State Key Laboratory of Functional Materials for Informatics, Shanghai Institute of Metallurgy, Chinese Academy of Sciences, 865 Changning Road, Shanghai 200050, China*
(Received 29 March 1999)

The magnetophonon resonance in the dc resistivity of a quasi-two-dimensional polar semiconductor irradiated by intense electromagnetic fields of terahertz frequency is investigated theoretically using a balance-equation approach. We find that the longitudinal resistivity as a function of the cyclotron frequency of the magnetic field exhibits, in addition to the conventional magnetophonon resonant peaks (zero-photon peak), many new peaks which correspond to one-, two-, and three-photon emission and absorption processes. With an increase of the strength of the terahertz field the zero-photon peaks descend, while the multiphoton ($|n|>1$) peaks ascend. These multiphoton-magnetophonon resonant peaks should be observed experimentally in realistic, high-mobility systems when exposed to an intense terahertz irradiation. [S0163-1829(99)07135-0]

Magnetophonon resonance[1] (MPR) in two-dimensional (2D) semiconductor systems has been extensively studied in the literature.[2–6] It arises generally from the resonant coupling between electrons and longitudinal-optic (LO) phonons and occurs when the separation between two Landau levels matches the LO-phonon energy. This effect leads to oscillation behavior in a variety of transport properties, such as magnetoresistance[6] and energy relaxation,[7] as functions of the magnetic field. In the presence of a high-frequency ac field, so far theoretical studies have been attempted only within the framework of linear-response theory. Xu and Zhang[8] calculated the frequency-dependent complex linear resistivity of a 2D electron system subject to a quantized magnetic field, based on a Drude-type formula proposed by Ting *et al.*,[9] and found that the effect of an ac field is to shift the positions of the resonant peaks of the real part of the longitudinal magnetoresistivity down from $M\omega_c=\Omega_{\rm LO}$ ($\omega_c$ and $\Omega_{\rm LO}$ are, respectively, the cyclotron and the LO-phonon frequency, $M=1,2,\ldots$ is an index difference between two Landau levels) to $M\omega_c+\omega=\Omega_{\rm LO}$ ($\omega$ is the frequency of the ac field), without a significant shape change of the resistivity curve.

The development of the free-electron laser technique, which provides a tunable source of linearly polarized far-infrared or terahertz (THz) electromagnetic radiation of high intensity, has recently stimulated extensive experimental and theoretical studies on the nonlinear dynamics of 2D electron systems driven by intense terahertz electric fields.[10–14] When a magnetically quantized 2D polar semiconductor is exposed to an intense electromagnetic radiation of THz frequency, the magnetophonon resonance behavior is expected to be affected drastically by the radiation field due to multiphoton emission and absorption. These interesting phenomena, however, cannot be disclosed within a linear-response theory.

The purpose of the present paper is to investigate the magnetophonon resonance in dc longitudinal magnetoresistivity in a 2D semiconductor system subject to an intense terahertz field, using the nonlinear balance-equation approach[14] extended to the case in the presence of a quantized magnetic field,[15] with all orders of multiphoton processes included.

We consider a two-dimensional system, which consists of $N_s$ electrons moving in the $x$-$y$ plane with a parabolic energy spectrum $\varepsilon(\mathbf{k}_\parallel)=k_\parallel^2/2m$ [$\mathbf{k}_\parallel\equiv(k_x,k_y)$]. A uniform magnetic field $\mathbf{B}=(0,0,B)$ applied along the $z$ axis quantizes these 2D electrons to form Landau levels of equidistance:

$$\varepsilon_n=(n+1/2)\omega_c, \quad n=0,1,2,\ldots \tag{1}$$

where $\omega_c=|eB|/m$ is the cyclotron frequency. When a uniform dc electric field $\mathbf{E}_0$ and a sinusoidal terahertz ac field of amplitude $\mathbf{E}_\omega$ and angular frequency $\omega$,

$$\mathbf{E}(t)=\mathbf{E}_0+\mathbf{E}_\omega\sin(\omega t), \tag{2}$$

are applied in the $x$-$y$ plane, the average drift velocity of the electrons in the time-dependent steady state, $\mathbf{v}_0$, can be determined by the following force and energy balance equations:[14,15]

$$0=N_s e\mathbf{E}_0+N_s e(\mathbf{v}_0\times\mathbf{B})+\mathbf{F}, \tag{3}$$

$$0=-\mathbf{v}_0\cdot\mathbf{F}-W+S_p. \tag{4}$$

Here $\mathbf{F}$ is the frictional force (due to electron-impurity and electron-phonon interactions), $W$ is the energy-transfer rate from the electron system to the phonon system due to electron-phonon interaction under the influence of the high-frequency electric field, and $S_p$ is the rate of the energy the electron system gains from the radiation field through the multiphoton absorption and emission process ($n=\pm1,\pm2,\ldots$) associated with the intraband transition of the electrons with the assistance of electron-impurity and electron-phonon interactions. They take exactly the same form as those without a magnetic field,[14,15] except that $\Pi_2(\mathbf{q}_\parallel,\Omega)$ now represents the imaginary part of the Fourier representation of the density correlation function for 2D electrons in the presence of the magnetic field, which can be written in terms of the density correlation function in the Landau representation[9,16]

$$\Pi_2(\mathbf{q}_\parallel,\Omega)=\frac{1}{2\pi l^2}\sum_{n,n'}C_{n,n'}(l^2q_\parallel^2/2)\Pi_2(n,n',\Omega), \tag{5}$$

$$\Pi_2(n,n',\Omega)=-\frac{2}{\pi}\int d\varepsilon[f(\varepsilon)-f(\varepsilon+\Omega)]\times{\rm Im}\,G_n(\varepsilon+\Omega){\rm Im}\,G_{n'}(\varepsilon), \tag{6}$$

 

where $l=\sqrt{1/|eB|}$ is the magnetic length,

$$C_{n,n+l}(Y)=[\,n!/(n+l)!\,]\,Y^l e^{-Y}[L_n^l(Y)]^2 \tag{7}$$

with $L_n^l(Y)$ being the associate Laguerre polynomial, $f(\varepsilon)=\{\exp[(\varepsilon-\mu)/T_e]+1\}^{-1}$ is the Fermi-distribution function, and $\mathrm{Im}\,G_n(\varepsilon)$ is the imaginary part of the Green's function of the Landau level $n$, which is proportional to the density of states, such that the sheet density of electrons is given by

$$N_s=-\frac{1}{\pi^2 l^2}\sum_n \int d\varepsilon\; f(\varepsilon)\,\mathrm{Im}\,G_n(\varepsilon). \tag{8}$$

This equation determines the chemical potential.

In principle, the $\mathrm{Im}\,G_n(\varepsilon)$ function in Eq. (6) should be determined self-consistently from the Dyson equation for Green's function and that for self-energy with all the scattering mechanisms included. The resultant imaginary part of the self-energy is generally a complicated function of the magnetic field, temperature, and Landau-level index, also dependent on the relative strength of the impurity and optical-phonon scattering. In the present study we do not attempt a self-consistent calculation of $G_n(\varepsilon)$. Instead, we use a Lorentz-type function for the Landau-level shape

$$\mathrm{Im}\,G_n(\varepsilon)=-\frac{\Gamma_n}{\Gamma_n^2+(\varepsilon-\varepsilon_n)^2} \tag{9}$$

with a unified broadening parameter $\Gamma_n=\Gamma$ for all the Landau levels, which is taken as $\Gamma=(2\omega_c\Gamma_0/\pi)^{1/2}$ with $\Gamma_0$ being related to the linear mobility $\mu_0$ in the absence of the magnetic field: $\Gamma_0=e/\mu_0 m$.[19] By considering the $\delta$ function like $\mathrm{Im}\,G_n(\varepsilon)$, the integration in Eq. (6) may be carried out, and the function $\Pi_2(n,n',\omega)$ takes the form[2]

$$\Pi_2(n,n',\omega)=-[f(\varepsilon_n-\omega)-f(\varepsilon_n)]\frac{4\Gamma}{4\Gamma^2+(\varepsilon_{n'}-\varepsilon_n+\omega)^2}. \tag{10}$$

In the case of a small dc field we can take the limit $\mathbf{v}_0\to 0$. The energy-balance equation (4) is reduced to[14]

$$\begin{aligned}0=&\sum_{\mathbf{q}_\parallel}|U(\mathbf{q}_\parallel)|^2\sum_{n=-\infty}^{\infty}J_n^2(\mathbf{q}_\parallel\cdot\mathbf{r}_\omega)\,n\omega\,\Pi_2(\mathbf{q}_\parallel,-n\omega)\\&+2\sum_{\mathbf{q},\lambda}|M(\mathbf{q},\lambda)|^2\sum_{n=-\infty}^{\infty}(n\omega-\Omega_{\mathbf{q}\lambda})J_n^2(\mathbf{q}_\parallel\cdot\mathbf{r}_\omega)\\&\times\Pi_2(\mathbf{q}_\parallel,\Omega_{\mathbf{q}\lambda}-n\omega)\left[n\left(\frac{\Omega_{\mathbf{q}\lambda}}{T}\right)-n\left(\frac{\Omega_{\mathbf{q}\lambda}-n\omega}{T_e}\right)\right].\end{aligned} \tag{11}$$

The force-balance equation yields the transverse and longitudinal parts of the resistivity tensor as

$$\rho_{xy}=B/N_s e, \tag{12}$$

and ($\mathbf{v}_0$ is assumed to be in the $x$ direction)

$$\begin{aligned}\rho_{xx}=&-\frac{1}{N_s^2e^2}\sum_{\mathbf{q}_\parallel}q_x^2|U(\mathbf{q}_\parallel)|^2\sum_{n=-\infty}^{\infty}J_n^2(\mathbf{q}_\parallel\cdot\mathbf{r}_\omega)\left[\frac{\partial}{\partial\Omega}\Pi_2(\mathbf{q}_\parallel,\Omega)\right]_{\Omega=-n\omega}+\frac{2}{N_s^2e^2}\sum_{\mathbf{q},\lambda}q_x^2|M(\mathbf{q},\lambda)|^2\\&\times\sum_{n=-\infty}^{\infty}J_n^2(\mathbf{q}_\parallel\cdot\mathbf{r}_\omega)\left\{\frac{1}{T_e}n'\left(\frac{\Omega_{\mathbf{q}\lambda}-n\omega}{T_e}\right)\Pi_2(\mathbf{q}_\parallel,\Omega_{\mathbf{q}\lambda}-n\omega)+\left[n\left(\frac{\Omega_{\mathbf{q}\lambda}-n\omega}{T_e}\right)-n\left(\frac{\Omega_{\mathbf{q}\lambda}}{T}\right)\right]\left[\frac{\partial}{\partial\Omega}\Pi_2(\mathbf{q}_\parallel,\Omega)\right]_{\Omega=\Omega_{\mathbf{q}\lambda}-n\omega}\right\}.\end{aligned} \tag{13}$$

In Eqs. (11) and (13), $U(\mathbf{q}_\parallel)$ stands for the electron-impurity potential, $M(\mathbf{q},\lambda)$ the electron-phonon matrix element in the plane-wave representation (the phonon is characterized by a three-dimensional wave vector $\mathbf{q}$ and a branch index $\lambda$, having energy $\Omega_{\mathbf{q}\lambda}$), $n(x)\equiv[\exp(x)-1]^{-1}$ is the Bose function, $T_e$ is the electron temperature, $\mathbf{r}_\omega\equiv e\mathbf{E}_\omega/(m\omega^2)$, and $J_n(x)$ is the Bessel function of the order $n$.

We see that the transverse resistivity has the same form as the conventional Hall resistivity in the absence of the high-frequency field. However, the longitudinal resistivity can be significantly affected by the strength and the frequency of the THz field.

As an example, we consider a GaAs/$Al_xGa_{1-x}$As heterojunction with electron density $N_s=2.0\times10^{15}$ m$^{-2}$ and the depletion charge density $N_d=5.0\times10^{14}$ m$^{-2}$. The electron effective mass $m=0.067m_0$ ($m_0$ is the free-electron mass). In addition to the impurity scattering, which is assumed to be weak, we consider only the polar optical- (LO-) phonon scattering via Fröhlich interaction with electrons. The LO-phonon energy $\Omega_{\mathrm{LO}}=36.6$ meV, the static dielectric constant $\kappa=12.9$, and the optical dielectric constant $\kappa_\infty=10.8$. In the numerical calculation we will use Eq. (10) for the $\Pi_2(\mathbf{q}_\parallel,\Omega)$ function and choose three different values of $\Gamma_0$: 0.058, 0.087, and 0.17 meV, which correspond to the electron mobility $\mu_0=30$, 20, and 10 m$^2$/V s, respectively.

Without the irradiation of the THz field, we have conventional magnetophonon resonance, as shown in Fig. 1, where the longitudinal magnetoresistivity due to optic phonon scattering, $\rho_{xx}$, is plotted as a function of $\omega_c/\Omega_{\mathrm{LO}}$ at lattice temperature $T=120$ K for the above-mentioned three different values of parameter $\Gamma_0$. Resonant oscillation of magnetoresistivity shows up with $\rho_{xx}$ peaking when the energy distance between the centers of two different Landau levels matches approximately the optic phonon energy $\Omega_{\mathrm{LO}}$, i.e., when the condition $M\omega_c=\Omega_{\mathrm{LO}}$ is almost satisfied ($M=1,2,\ldots$ represents an index difference of two Landau levels). The $\Gamma_0=0.17$ meV case is roughly comparable with the oscillation part of the experimentally observed magnetoresistivity[6,17,18] for high low-temperature mobility ($\sim$100 m$^2$/V s) GaAs/$Al_xGa_{1-x}$As systems having an electron sheet density of order of $2\times10^{15}$ m$^{-2}$.

In the presence of a THz field, we see from Eq. (10) that the $\Pi_2(\mathbf{q}_\parallel,\Omega_{\mathrm{LO}}-n\omega)$ function has local maxima under the condition

$$M\omega_c+n\omega=\Omega_{\mathrm{LO}}. \tag{14}$$

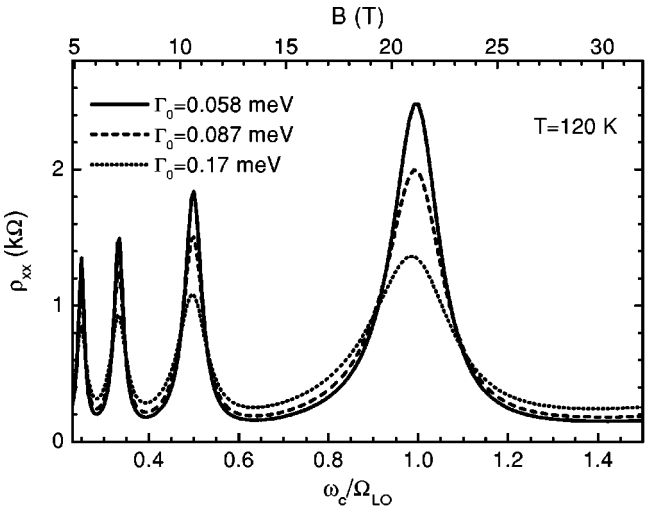


FIG. 1. Magnetophonon resonance in the longitudinal resistivity $\rho_{xx}$ for three different values of the Landau-level broadening parameter $\Gamma_0$: 0.058, 0.087, and 0.17 meV.

Therefore, it may happen that the longitudinal resistivity [Eq. (13)], as well as other transport quantities, also exhibit maxima or other kinds of structure around where the condition (14) is approximately satisfied. Here $n=0,\pm1,\pm2,\ldots$ corresponds to the zero-photon, one-photon, and two-photon emission and absorption process, respectively. In the numerical calculation, we first consider the parallel configuration, i.e., the THz electric field polarizes along the direction parallel to $\mathbf{v}_0$. To demonstrate the fine structure related to the multiphoton process, we first calculate the longitudinal resistivity under the influence of THz radiation fields having three different angular frequencies, $\omega=0.1\Omega_{LO}$, $0.15\Omega_{LO}$, and $0.2\Omega_{LO}$ (or frequency $\nu=\omega/2\pi=0.89$, 1.34, and 1.78 THz) and three different amplitudes $E_\omega=0.5$, 0.75, and 1 kV/cm, by using a small value $\Gamma_0=0.058$ meV. The lattice temperature is $T=120$ K. The calculated resistivity $\rho_{xx}$ is shown as a function of $\omega_c/\Omega_{LO}$ in Fig. 2. The zero-photon and all possible multiphoton peaks in the cases $M=1$ and 2 are displayed and identified by two integers: $(M,n)$. The following features can be seen. (1) Zero-photon peaks (1,0) and (2,0) are located essentially at the same positions as in the case of the magnetophonon resonance without a THz field (Fig. 1), but the heights of the $\rho_{xx}$ resonant peaks are significantly reduced due to the irradiation of the THz field. (2) In the case of $\omega/2\pi=0.89$ THz [Fig. 2(a)], with an increase of the THz-field amplitude $E_\omega$ from 0.5 to 1.0 kV/cm, zero-photon peaks (1,0) and (2,0) and one-photon peaks with $M=1$, (1,1) and (2,1), descend, while two-, three-, and four-photon peaks, (1,2), (1,3), (1,−2), (1,−3), (1,−4), and (2,−2), and one-photon peaks with $M=2$, (2,1) and (2,−1), ascend [Fig. 2(a)]. In the cases of $\omega/2\pi=1.34$ THz [Fig. 2(b)] and $\omega/2\pi=1.78$ THz [Fig. 2(c)], however, all the nonzero-photon peaks are enhanced when the strength of the THz field increases. (3) For a fixed THz-field amplitude, this effect of resonant peaks descending or ascending appears stronger at a lower frequency of the THz field than at a higher frequency [Figs. 2(a)–2(c)], just as that of the THz-field-induced suppression or enhancement of the dc mobility is stronger at lower frequency.[14] (4) The widths of all the resonant peaks having the same index $M$, such as (1,0), (1,1), (1,−1), (1,2), (1,−2), (1,3), (1,−3), and (1,−4), are essentially the same but differ from those having different $M$. This feature can be used to distinguish the close multiphoton peaks with different $M$, such as (1,3) and (2,−2) in Fig. 2(a).

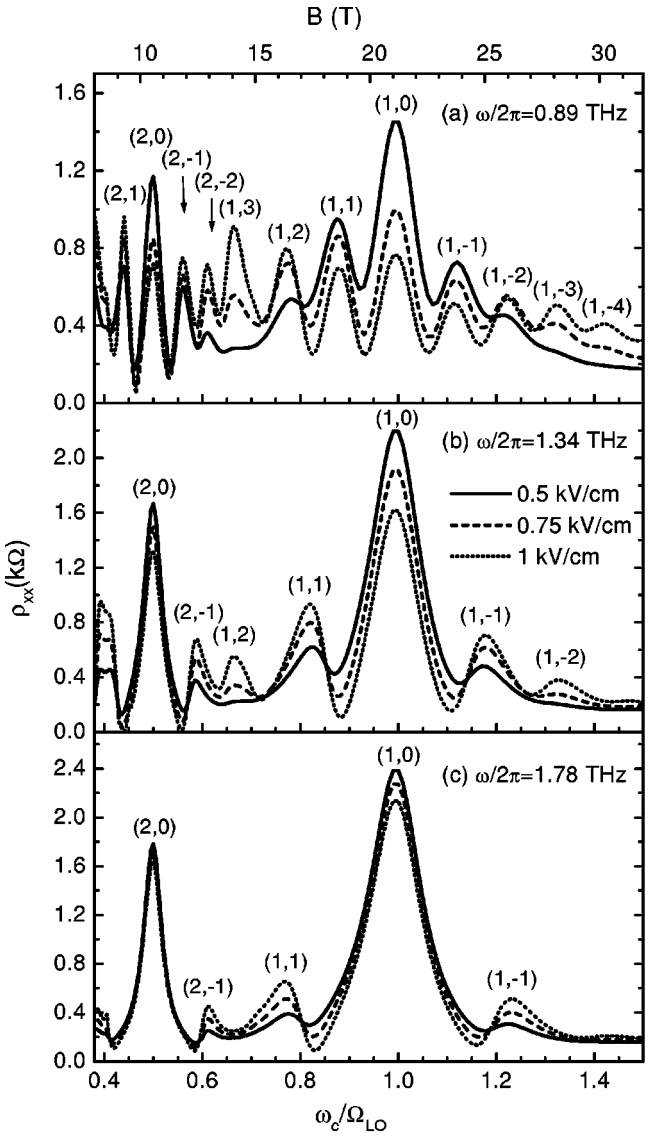


FIG. 2. Multiphoton-magnetophonon resonance in the longitudinal resistivity $\rho_{xx}$ of a GaAs/$Al_xGa_{1-x}$As heterojunction driven by radiation fields having three different frequencies, (a) $\nu=\omega/2\pi=0.89$, (b) 1.34, (c) 1.78 THz, and three different amplitudes $E_\omega=0.5$, 0.75, and 1 kV/cm. The peaks are indicated by two integers $(M,n)$ in reference to the resonant condition (14). The value of parameter $\Gamma_0$ is 0.058 meV. The lattice temperature $T=120$ K.

The multiphoton resonant peaks can also be observed if, for a fixed magnetic field, we look at the magnetoresistivity as a function of frequency of the THz field. Figure 3 is obtained at $T=120$ K under the condition of a given amplitude of the THz field $E_\omega=0.5$ kV/cm for the broadening parameter $\Gamma_0$ as in Fig. 2. Multiphoton peaks appear clearly.

Figure 4 shows the multiphoton-magnetophonon resonance in the longitudinal resistivity $\rho_{xx}$ of the same GaAs/$Al_xGa_{1-x}$As heterojunction driven by radiation fields having three different amplitudes $E_\omega=0.5$, 0.75, and 1.0 kV/cm but the same frequency $\omega/2\pi=0.89$ THz, obtained at lattice temperature $T=120$ K by using a larger broadening parameter $\Gamma_0=0.17$ meV. This $\Gamma_0$ corresponds to a mobility

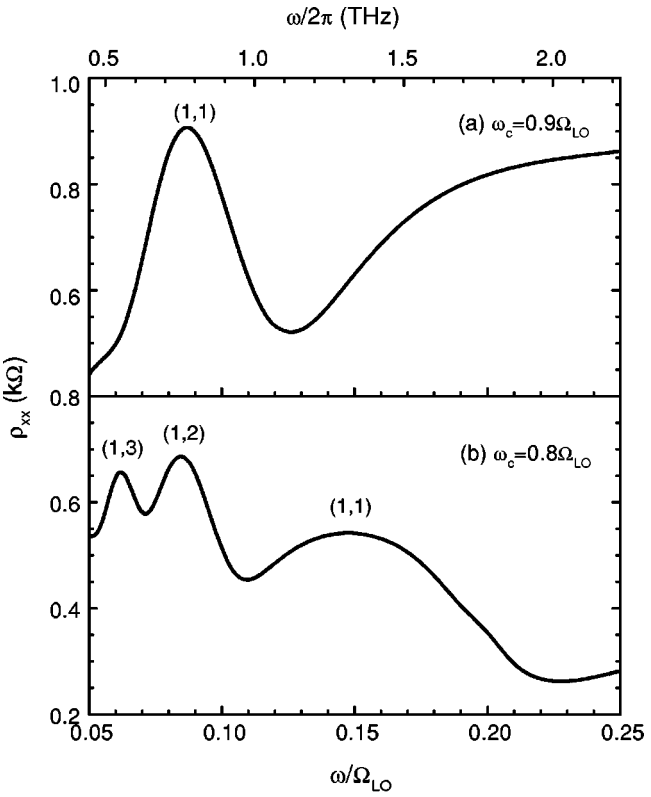


FIG. 3. Resistivity $\rho_{xx}$ versus the frequency of the THz field for two different strengths of magnetic field: (a) $\omega_c/\Omega_{\rm LO}=0.9$ and (b) 0.8. The amplitude of the THz field $E_\omega=0.5$ kV/cm, the broadening parameter $\Gamma_0=0.058$ meV, and the lattice temperature $T=120$ K.

of $\mu_0=10$ m$^2$/Vs when estimated with $\mu_0=e/m\Gamma_0$. It is a quite realistic situation for GaAs/$Al_xGa_{1-x}$As heterojunctions even $\mu_0$ is taken as the mobility at $T=120$ K. The multiphoton resonant peaks, although not as sharp as in the case of $\Gamma_0=0.058$ meV, still show up distinctly in this figure. All the features discussed with respect to Fig. 2 remain. The overall shape of the $\rho_{xx}$-vs-$\omega_c/\Omega_{\rm LO}$ curve appears quite different for different strengths of the radiation field. These multiphoton-magnetophonon resonant peaks should be observed experimentally in a moderately high-mobility GaAs/$Al_xGa_{1-x}$As heterojunction irradiated by an intense THz irradiation.

We have also performed a numerical calculation in the perpendicular configuration, i.e., the high-frequency field polarizes along the direction perpendicular to $\mathbf{v}_0$. Qualitatively

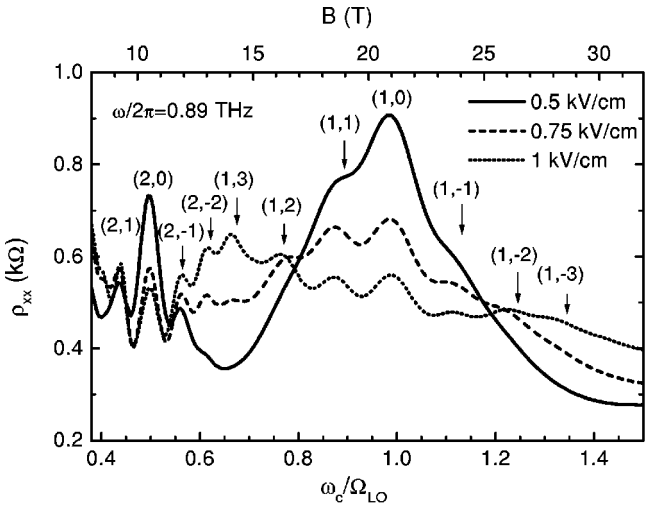


FIG. 4. Longitudinal resistivity $\rho_{xx}$ as a function of the strength of the magnetic field for three different amplitudes of the THz field, $E_\omega=0.5$, 0.75, and 1 kV/cm. The broadening parameter $\Gamma_0=0.17$ meV, the frequency of the THz field $\omega/2\pi=0.89$ THz, and the lattice temperature $T=120$ K.

similar features are obtained. However, to achieve a quantitatively comparable effect, a larger strength of the THz field is needed in the perpendicular case than in the parallel case.

Multiphoton-magnetophonon resonance peaks can also show up in the electron temperature $T_e/T$ versus $\omega_c/\Omega_{\rm LO}$. However, at the strengths of the THz fields discussed above, the maximum oscillating amplitude of $T_e/T$ is only a few percent, and thus hardly observable in the present situation.

In conclusion, we have demonstrated that when a magnetically quantized 2D polar system is exposed to an intense electromagnetic radiation of THz frequency, the magnetophonon resonant peaks may appear in the longitudinal dc resistivity as a function of the magnetic field (for fixed frequency and the amplitude of the radiation field), and may also show up in the longitudinal dc resistivity as a function of the frequency of the radiation field (for fixed strength of the magnetic field and fixed amplitude of the radiation field). We expect that these predictions about the behavior of multiphoton-magnetophonon resonance can be confirmed experimentally.

This work was supported by the National Natural Science Foundation of China, the Ministry of Science and Technology of China, the Shanghai Municipal Commission of Science and Technology, and the Shanghai Foundation for Research and Development of Applied Materials.

[1] V. L. Gurevich and Yu. A. Firsov, Zh. Éksp. Teor. Fiz. **40**, 199 (1961) [Sov. Phys. JETP **13**, 137 (1961)].
[2] R. Lassnig and W. Zawadzki, J. Phys. C **16**, 5435 (1983).
[3] P. Warmenbol *et al.*, Phys. Rev. B **37**, 4694 (1988).
[4] P. Vasilopoulos, Phys. Rev. B **33**, 8587 (1986).
[5] N. Mori *et al.*, J. Phys. C **21**, 1791 (1988).
[6] R. J. Nicholas, in *Landau Level Spectroscopy*, edited by G. Landwehr and E. I. Rashba (Elsevier, Amsterdam. 1991), p. 777.
[7] Xiaoguang Wu and F. M. Peters, Phys. Rev. B **55**, 9333 (1997).
[8] W. Xu and C. Zhang, Phys. Rev. B **54**, 4907 (1996).
[9] C. S. Ting *et al.*, Phys. Rev. B **16**, 5394 (1977).
[10] N.G. Asmar *et al.*, Phys. Rev. B **51**, 18 041 (1995).
[11] N. G. Asmar *et al.*, Appl. Phys. Lett. **68**, 829 (1996).
[12] A. G. Markelz *et al.*, Appl. Phys. Lett. **69**, 3975 (1996).
[13] W. Xu, Phys. Rev. B **57**, 12 939 (1998); **57**, 15 282 (1998).
[14] X. L. Lei, J. Appl. Phys. **84**, 1396 (1998); J. Phys.: Condens. Matter **10**, 3201 (1998).
[15] X. L. Lei and S. Y. Liu, Eur. Phys. J. B (to be published).
[16] W. Cai *et al.*, Phys. Rev. B **31**, 4070 (1985).
[17] D. R. Leadley *et al.*, Phys. Rev. B **48**, 5457 (1993).
[18] P. M. Koenraad *et al.*, Physica B **256-268**, 268 (1998).
[19] T. Ando, J. Phys. Soc. Jpn. **38**, 989 (1975).